LA-UR -82-1882

Conf-820718--2

Los Alamos National Laboratory is operated by the University of California for the United States Department of Energy under contract W-7405-ENG-36.

LA-UR--82-1882

DE82 017593

TITLE: A HIGH-INTENSITY NEUTRINO FACILITY AT LAMPF

AUTHOR(S): Howard S. Matis, Lewis Agnew, Thomas J. Bowles, Robert L. Burman, Richard K. Cooper, Thomas W. Dombeck, Robert J. Macek, and Gerard J. Stephenson, Jr.

SUBMITTED TO: XXI International Conference on High Energy Physics, Paris, France, July 26-30, 1982.

Los Alamos National Laboratory
Los Alamos, New Mexico 87545

A HIGH-INTENSITY NFUTRINO FACILITY AT LAMPF

Howard S. Matis, Lewis Agnew, Thomas J. Bowles, Robert L. Burman,
Richard K. Cooper, Thomas W. Dombeck, Robert J. Macek,
and Gerard J. Stephenson, Jr.

Los Alamos National Laboratory, Los Alamos, NM 87545

ABSTRACT

A high-intensity neutrino facility is being proposed to be built at LAMPF. This facility, which uses 100 μA of protons at 800 MeV incident upon a graphite target, will be run in two modes. The first mode will use the usual 750-μs pulse width at 12 Hertz at LAMPF. The second one will use the Proton Storage Ring (PSR), currently under construction, and compress the proton bursts to 0.270 μs. In this mode, pure beams of high-intensity neutrinos and antineutrinos will be created. Using this facility, one can achieve very sensitive limits on neutrino oscillations and a precise measurement of neutrino-electron scattering. In addition, there are many other interesting neutrino scattering reactions to study.

A low energy and high intensity neutrino facility[1] has been designed for the Los Alamos Meson Physics Facility (LAMPF). This facility will provide intense time-separated neutrino beams from the primary beam at LAMPF. From LAMPF, 100 μA of 800-MeV protons will strike a target and produce pions that will be magnetically focused for increased intensity as well as sign selection. Thus pure beams of high intensity muon neutrinos and muon antineutrinos will be provided. For most applications, the protons will pass through the Proton Storage Ring (PSR) now under construction,[2] and will be spilled on the production target in 270-ns bursts at 12 Hz that will provide background suppression and allow separation of electron neutrinos from muon neutrinos by timing. This facility is designed to accommodate experiments searching for neutrino oscillations, experiments using ν_μ or $\bar{\nu}_\mu$'s from pion decay in flight, and experiments using ν_μ and/or $\bar{\nu}_\mu$ and ν_e from a beam stop source. In addition, room has been left to allow for future additions that might include an additional beam line or a device to store muons from pion decay in order to provide a source of high-energy ν_e's from muon decay.[3]

The beam transport system at the neutrino facility is designed to allow multiplexed operation of at least 200 μA of beam at LAMPF, both with and without the PSR. Figure 1 shows the extraction of the beam from LAMPF and and Fig. 2 shows the layout of the beam transport system. When the PSR is in use, beam is extracted in the usual manner and deflected by a kicker-septum magnet system into the neutrino beam line. Multiplexed operations of the beam, when the PSR is not operating, can be done on a pulse-by-pulse basis using the kicker magnet to be installed in Line D to deflect pulses into the neutrino beam line. In either running condition, up to 100 μA of beam can be provided to Target Cell 1 at the existing

neutron scattering facility, while at least 100 μA of beam can simultaneously be provided to the neutrino facility.

The proton beam is focused onto the neutrino-production target in one of three modes:

(1) the beam is focused onto a 3-cm-diameter, 40-cm-long carbon production target that is followed by a 30-m-long pion decay channel,

(2) the carbon production target is moved on rails further down the pion decay channel and beam pipe with two quadrupole doublets is installed. The beam is then focused onto the carbon production target, which is followed by a 12-m-long (or 10 m) decay channel,

(3) the carbon production target is removed and the water-copper beam stop at the end of the decay channel serves as the neutrino source.

Figure 3 shows a layout of the neutrino beam line and the nearby experimental areas.

The pion-production target will be graphite of a design similar to the Biomed target that has been in use for many years at LAMPF.[4] We anticipate two running conditions for the proton beam on target: (1) the transporting of macro-pulses directly from the LAMPF linac, and (2) the transporting of the wider divergence beam from the PSR. In the first case we can expect proton spot sizes ~2 mm FWHM and can use thin-diameter targets of ~5 mm. The PSR running conditions yield a broader spot size, ~1.2 cm FWHM, requiring a 3-cm-diameter target to contain the beam. As most of the anticipated experiments will be carried out using the PSR, this larger diameter target has been used in the following calculations on the expected neutrino flux.

A major uncertainty in calculating the neutrino flux comes from the lack of knowledge of the pion yields from such a target. Pion-yield cross sections have been measured at LAMPF, TRIUMF, SIN and BNL for various targets and incident proton energies from 580 to 1000 MeV.[5-10] The most complete published yield data are at 730 MeV by Cochran et al.,[7] having errors ~5% to 10%. These have been augmented by recent experiments at LAMPF that have taken data at 730 MeV.[11] Also, data were recently taken on π^+ yields at 800 MeV for a series of angles from 7^o to 45^o.[12] These results were used in our flux calculations.

The neutrino flux can be greatly enhanced by focusing the pions into the decay channel toward the detector. A possible design is a dipole magnet. It will consist of a large gap (50 cm) magnet with a 12-kG field. The magnet will be positioned just downstream of the target. The pole pieces are arranged symmetrically about the target axis with the field reversed in the lower section. The trajectories through the magnet are such that pions of one charge state will exit approximately parallel to the decay tunnel axis for all pion production angles within the forward 60^o cone. The other charged state will be defocused. The total solid angle subtended by the magnet is about 1.5 sr.

An alternative focusing device is a magnetic horn. The difficulty with its use is that it would have to be pulsed 10 times faster than other horns have been operated. Because of its advantages in focusing we are actively investigating possible horn designs.

To calculate the neutrino flux, a Monte Carlo program[13] was written assuming a dipole magnet for the focusing device. With this code one calculates that a decay channel length of 12 m will produce 4×10^6 ν/cm^2-s on a 100 μA proton current with an average neutrino energy of 150 MeV. The

corresponding energy spectrum for this case is shown in Fig. 4. The $\bar{\nu}_\mu$ flux, also shown on that figure, has an intensity of 1×10^6 $\bar{\nu}/cm^2$-s and has an average energy of 130 MeV. At much longer detector distances where the decay channel length does not affect the solid angle at the detector, such as for the oscillation experiments, a 30-m decay channel length is more desirable. This configuration yields a factor of two more neutrino flux over the 12-m decay length.

We have the capability of adjusting the neutrino-energy spectrum and shifting the peak by at least 50 MeV. This can be accomplished by (1) lowering the proton energy coming out of LAMPF, (2) adjusting the dipole current, and (3) placing plugs downstream from the target to specifically absorb certain pion components out of the beam before they can decay. This energy adjustment capability may be important for reducing or determining backgrounds and for obtaining two separate energy measurements that could be useful in the neutrino oscillation experiment. In neutrino-electron scattering adjusting the ν_μ spectrum to overlap the $\bar{\nu}_\mu$ spectrum may eliminate a major source of uncertainty in the measurement of the Weinberg angle.

The results presented in Fig. 4 are representative of expected fluxes and have been used in this proposal to calculate event rates. The flux optimization has not been completed. Increasing the repetition rate of the ring, an improved focusing device, or an increased proton energy, can greatly improve the event rates.

Scaling the numbers from the current Line A beam stop (see Ref. 14) we find fluxes of each separate neutrino type (ν_μ, $\bar{\nu}_\mu$, ν_e) at a 6-m detector distance from the beam stop to be at least 9×10^6 ν/cm^2-s. The short time

structure of the PSR pulse will make it possible to distinguish ν_e and $\bar{\nu}_\mu$ neutrinos from muon decay, from the ν_μ neutrinos.

Both positive and negative pions are produced in the target, so the cleanliness of the resultant neutrino beams will depend on the effectiveness of the focusing device to bend the unwanted pions out of the line of flight to the detector. The Monte Carlo calculation was used to estimate the amount of the wrong-sign neutrinos that strike the detector. We found that in the ν_μ beam $\bar{\nu}_\mu/\nu_\mu = 0.005$. In the corresponding $\bar{\nu}_\mu$ beam we found $\nu_\mu/\bar{\nu}_\mu = 0.04$.

Muons from the pion decays can also produce a ν_e background. However, the muon decay length is ~200 times longer than for pions. After considering angular distributions along the 12-m long decay channel, we find a background $\nu_e/\nu_\mu = 0.001$. Also, the ν_e background energy spectrum peaks at 120 MeV as shown in Fig. 4, which is considerably lower than the ν_μ spectrum. The backgrounds of ν_e's are worse at high-energy accelerators due to an additional source from K_{e3} decays that is not present at LAMPF. ANL[15] found ~0.5% ν_e/ν_μ while CERN[16] had 0.2% to 3.0% contamination depending on the neutrino energy. Fermilab[22] estimates a 1.0% ν_e contamination.

In designing a detector that is suitable for the PSR facility, a few points are important to consider. The energies involved are low, so most often only one energetic charged track emerges from the vertex. Most often this single track is an electron or muon. Its detection is possible only if it travels through a sufficiently large number of tracking units in the detector. To achieve high detection efficiencies requires a segmentation much finer than at higher-energy accelerators. The detector must also

provide good particle type separation by dE/dX, range, or a particle decay signal.

A design of a detector in an experimental proposal to the facility[17] is shown in Fig. 5. There will be four drift chamber subunits in each module giving two X- andtwo Y- position coordinates per module. Pulse heights will also be recorded for each wire hit. Each module will have its own hodoscope bank to be used in the trigger.

Aluminum plates (5 m on a side and 1/4 cm thick) will be an integral part of the drift chamber structure forming its front and back walls. I-beams will be used as spacers to form the drift regions. Incorporating the aluminum into the drift chambers results in simple, rigid, and self-supporting construction. The drift region will be 1 cm in width and wires will be strung every 1.5 cm. The wires will alternate as cathode wires and sense wires. With this arrangement, the cathode wires will resolve the left-right ambiguity problem by making use of the fact that the induced signal is strongest on the side of the sense wire where the particle traversed (see Ref. 15).

The scintillator planes will be 2 cm thick with one 5-m x 5-m plane per module. Timing and proportional information will be recorded for each phototube in a fashion similar to the drift chamber wires, though in some cases we will want to register as many as three signals for a single event.

The detector will provide good muon and electron identification using decay timing and dE/dX information. Gamma rays will also be readily identified after their conversion to two electrons yielding a twice minimal dE/dX signal. Also, the deposited energy in the scintillator will give an estimate of the particle's kinetic energy.

The high detector granularity permits many coordinates to be registered on a track yielding good angle resolution. Even with the high granularity, the overall detector density is large (0.9 gm/cm^3). This is an important consideration at LAMPF energies because the rapid flux decrease along the length of the detector dictates as short a detector as possible to optimize event rates.

In order to discriminate against cosmic ray background striking the detector, it is necessary to detect cosmic rays. The neutrino events will generally be contained within a small region in the detector due to the small energies involved. Therefore, the use of an active cosmic-ray veto permits inclusion of almost all of the detector volume (~80%) into its fiducial region. We are anticipating that the outer 50 cm of the detector in each direction will be used as part of the cosmic-ray veto system.

The anticoincidence shield is composed of two layers (1-X and 1-Y) of drift chambers, or possibly scintillators, that completely surround the main detector, except underneath. The anticoincidence chambers may be of the same design as in the detector modules, but will not include proportional mode electronics. This counter would provide rejection efficiencies ~10^{-4} for charged particles, which is sufficient for the background levels expected. To provide rejection of electron events originating from stopped cosmic muons in the detector, the anticoincidence shield will be checked for a signal for periods up to 25 μsec before the event in the main detector, using a delayed coincidence measurement system similar to that being used in LAMPF Experiment 225.[16]

With the facility and detector described above, event rates can be calculated. These rates for 100 days of beam time are shown in Table I. For the reactions considered the number of detected neutrino events are

large, showing the richness of the facility. Furthermore, because of the low backgrounds due to the short time structure of this machine, excellent precision can be expected.

In fact, with this facility it will be possible to study with great sensitivity oscillation phenomena with a ν_μ beam. Using a 500-ton detector at 3800 m and another 20-ton detector at 200 meters, one can achieve extreme sensitivities to neutrino oscillations. The proposed location of those detectors relative to LAMPF is shown in Fig. 6. With this configuration we can achieve, at 90% confidence limits, an upper limit of $\Delta m^2 < 0.01(eV)^2$ for ν_μ disappearance and $0.001(eV)^2$ for the exclusive channel $\nu_\mu \rightarrow \nu_e$. These values are an order of magnitude better than anything proposed elsewhere. For large Δm^2, the experiment can set limits on the mixing angle of $\sin^2 2\theta = 0.17$ for ν_μ disappearance and 0.001 for $\nu_\mu \rightarrow \nu_e$. These limits should be compared to the current results and proposed experiments that are shown in Fig. 7.

Using a 500-ton detector at a position close to the production area, one can measure ν_μ-e and $\bar{\nu}_\mu$-e elastic scattering with sufficient precision to determine the fundamental coupling constants of the weak neutral current with an accuracy of a few percent and to make definite statements about the space-time structure of the neutral current. A unique measurement of the differential distribution is made possible by the relative wide angular distributions of electrons due to the low neutrino energies available at this facility. The purity and low energy of the neutrino beam are also crucial to reduce backgrounds and other systematic errors in this experiment.

Another unique feature of this facility is the availability of electron neutrinos separated from the muon neutrinos in time. The low duty factor will suppress cosmic-ray backgrounds to allow clean ν_e-e scattering experiments.

Furthermore, this facility will also allow the study of neutrino-nucleus scattering. In particular, at the low-momentum transfers available, one may study individual inelastic transitions where the nuclear states provide unique selectivity, especially with regard to the isospin structure of the charged and neutral currents. With both muon and electron neutrinos available, one will be able to conduct detailed tests of universality. The availability of high-intensity muon neutrino and muon antineutrino beams will make tests of CP violation possible.

The design for this facility has benefited from many contributions by F. Boehm, R. McKeown, and P. Nemethy. We thank them for their assistance.

TABLE I

SELECTED EVENT RATES EXPECTED IN DETECTOR FOR 100 RUNNING DAYS

$\phi_\nu = 4 \times 10^6\ \nu/cm^2\text{-}s$

$\phi_{\bar{\nu}} = 1 \times 10^6\ \bar{\nu}/cm^2\text{-}s$

Detector composition: 365 tons of Al + 128 tons of $CH_{1.1}$ (scint.)

$\nu_\mu Al \rightarrow \mu^- + x$	680,000	$\nu_\mu C \rightarrow \mu^- + x$	224,000
$\bar{\nu}_\mu Al \rightarrow \mu^+ + x$	11,000	$\bar{\nu}_\mu C \ \mu^+ + x$	4,000
		$\bar{\nu}_\mu p \rightarrow \mu^+ + n$	56,000
		$\nu_\mu p \rightarrow \nu_\mu p$	1,900
		$\bar{\nu}_\mu p \rightarrow \bar{\nu}_\mu p$	180
$\nu_\mu e \rightarrow \nu_\mu e$	600	$\nu_\mu C \ \mu^- + N^{12}(\beta^+)$	16,000
$\bar{\nu}_\mu e \rightarrow \bar{\nu}_\mu e$	130	$\bar{\nu}_\mu C \rightarrow \mu^+ + B^{12}(\beta^-)$	800
$\nu_\mu C \rightarrow \nu_\mu C^*$ (15.11 MeV)	1,500		
$\bar{\nu}_\mu C \rightarrow \bar{\nu}_\mu C^*$ (15.11 MeV)	120		
$\nu_e e \rightarrow \nu_e e$ (beam stop at 9 m)	500		
$\nu_e Al \rightarrow e^- + X$ (beam stop at 9 m)	3,000		

REFERENCES

1. "A Proposal to the Department of Energy for a High-Intensity Los Alamos Neutrino Source," G. J. Stephenson,Jr., Chairman (1982).

2. "Study of Uses of a Proton Storage Ring," D. Nagle, ed., LA-7490-MS (1978).

3. "A Pion and Muon Magnetic Trap as a Source of Electron and Muon Neutrinos," V. M. Lobashev and D. V. Serdyuk, NIM, 136, 61 (1976).

4. L. Agnew et al., "Graphite Targets for Use in High-Intensity Beams at LAMPF," IEEE Trans. Nucl. Sci., Vol. NS-26, 4143 (1979).

5. W. Hirt, (thesis, unpublished, 1962); J. Crawford et al., PR C22, 1184 (1980).

6. P. W. James et al., VPN-75-1 (Preprint, TRIUMF, 1975).

7. D. Cochran et al.,PR D6, 3084 (1972).

8. R. Edge et al., N. Cim. 31A, 641 (1976).

9. R. D. Werbeck and R. J. Macek, IEEE Trans. on Nucl. Sci. NS-22, 1598 (1975).

10. Private communication, R. Frosch, SIN, June 15, 1981.

11. LAMPF Experiment 591 (R. DeVries and N. DiGiacomo, Spokesmen, 1980).

12. Extension to LAMPF Experiment 517 (J. Simmons, Spokesman, 1981).

13. T. Dombeck, "LANLNU--A Description of the Monte Carlo Calculation of the Neutrino Flux at the High-Intensity Los Alamos Neutrino Source," (Los Alamos National Laboratory Report LA-UR-82-1589, May 1982).

14. H. H. Chen, University of California at Irvine Internal Report UCI - Neutrino No. 44 (July 1980).

15. S. Barish et al., PR D16, 3103 (1977).

16. P. Musset and J.-P. Vialle, Phys. Rep. 39, 1 (1978).

17. T. Dombeck et al., LAMPF Proposal E-638.

18. J. Fischer et al., NIM 151, 451 (1978); A. H. Walenta, NIM 151, 460 (1978); and A. Breskin et al., NIM 151, 473 (1978). Chambers using this technique have been operated successfuly; for example see G. Atencio et al., NIM 187, 381 (1981).

19. H. Chen et al., LAMPF Proposal E-225 (January 1977), and H. Chen, private communication on cosmic-ray induced neutron backgrounds.

FIGURE CAPTIONS

Fig. 1. Layout of proposed neutrino facility showing existing and proposed construction.

Fig. 2. Beam transport system of proposed facility showing extraction lines from PSR and Line D feeding new neutrino beam line.

Fig. 3. Layout of new construction proposed at end of Line D. The three target positions (30-m decay channel, 12-m decay channel, and water beam stop) are shown.

Fig. 4. The computed ν_μ and $\bar{\nu}_\mu$ energy spectra are shown. The total integrated fluxes are given for the optimal pion decay channel lengths and dipole focusing fields discussed in the text.

Fig. 5. Module for a possible 500-ton neutrino detector.

Fig. 6. Contour map of site of proposed neutrino facility and proposed 200-m and 3800-m detector buildings.

Fig. 7. The experimental sensitivity for proposed and completed experiments. The area to the right of the curve is excluded. Ref. 1 has the complete list of experiments.

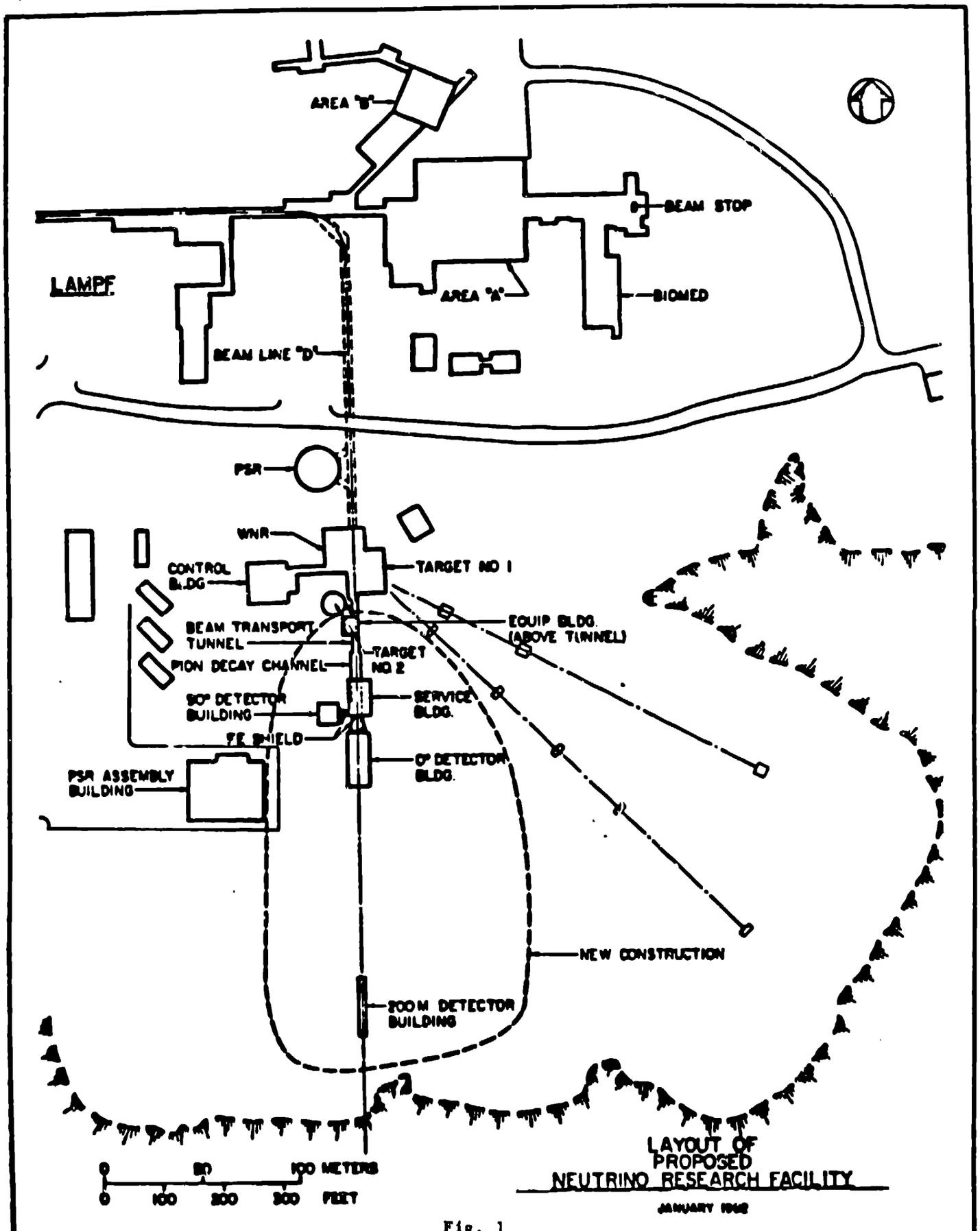
AREA "B"
BEAM STOP
LAMPF
AREA "A"
BIOMED
BEAM LINE "D"
PSR
WNR
CONTROL BLDG
TARGET NO 1
EQUIP BLDG. (ABOVE TUNNEL)
BEAM TRANSPORT TUNNEL
TARGET NO 2
PION DECAY CHANNEL
90° DETECTOR BUILDING
SERVICE BLDG.
FE SHIELD
0° DETECTOR BLDG.
PSR ASSEMBLY BUILDING
NEW CONSTRUCTION
200M DETECTOR BUILDING
0 50 100 METERS
0 100 200 300 FEET
LAYOUT OF PROPOSED NEUTRINO RESEARCH FACILITY
JANUARY 1968

Fig. 1

NEUTRINO FACILITY BEAM TRANSPORT

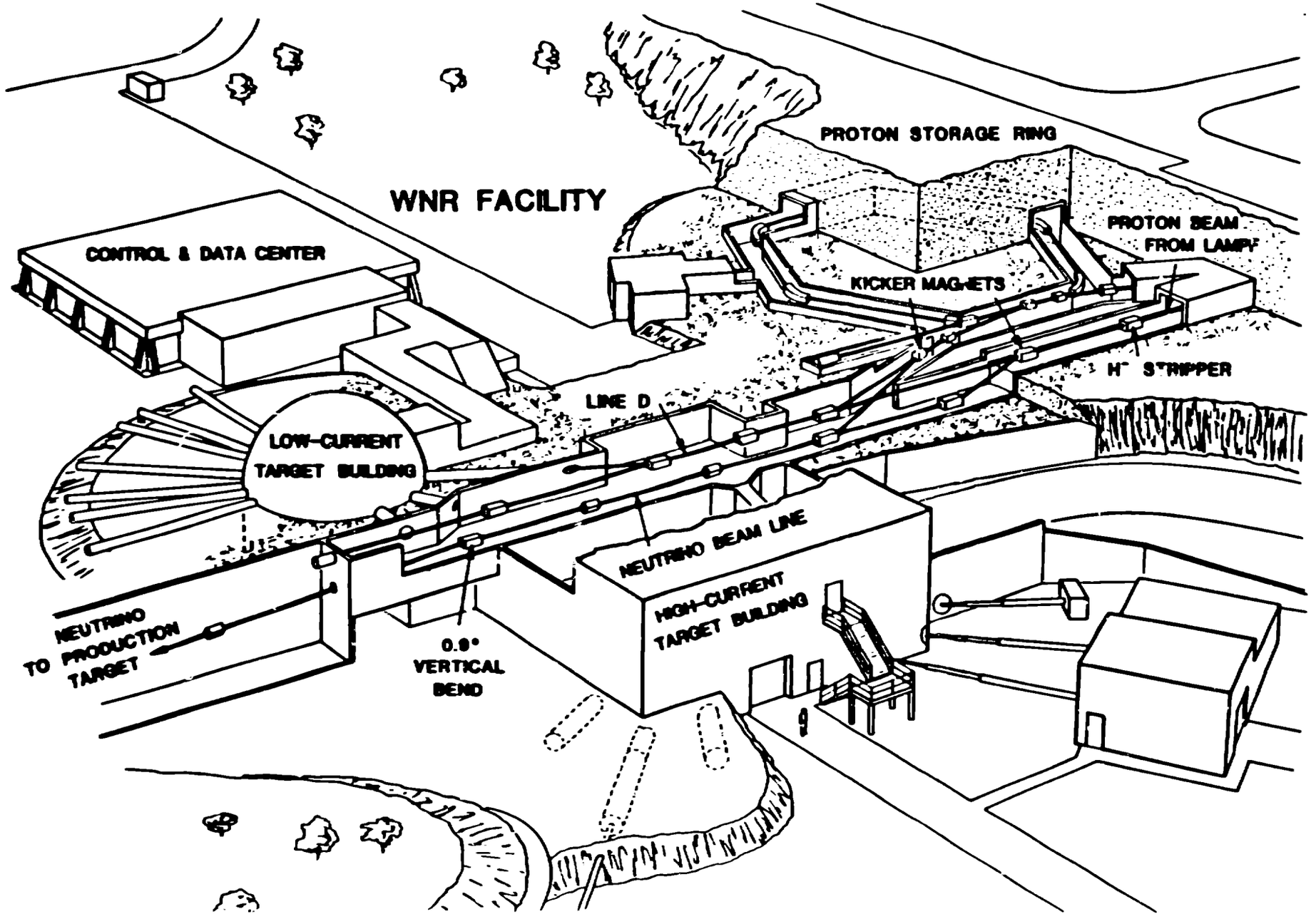

Fig. 2

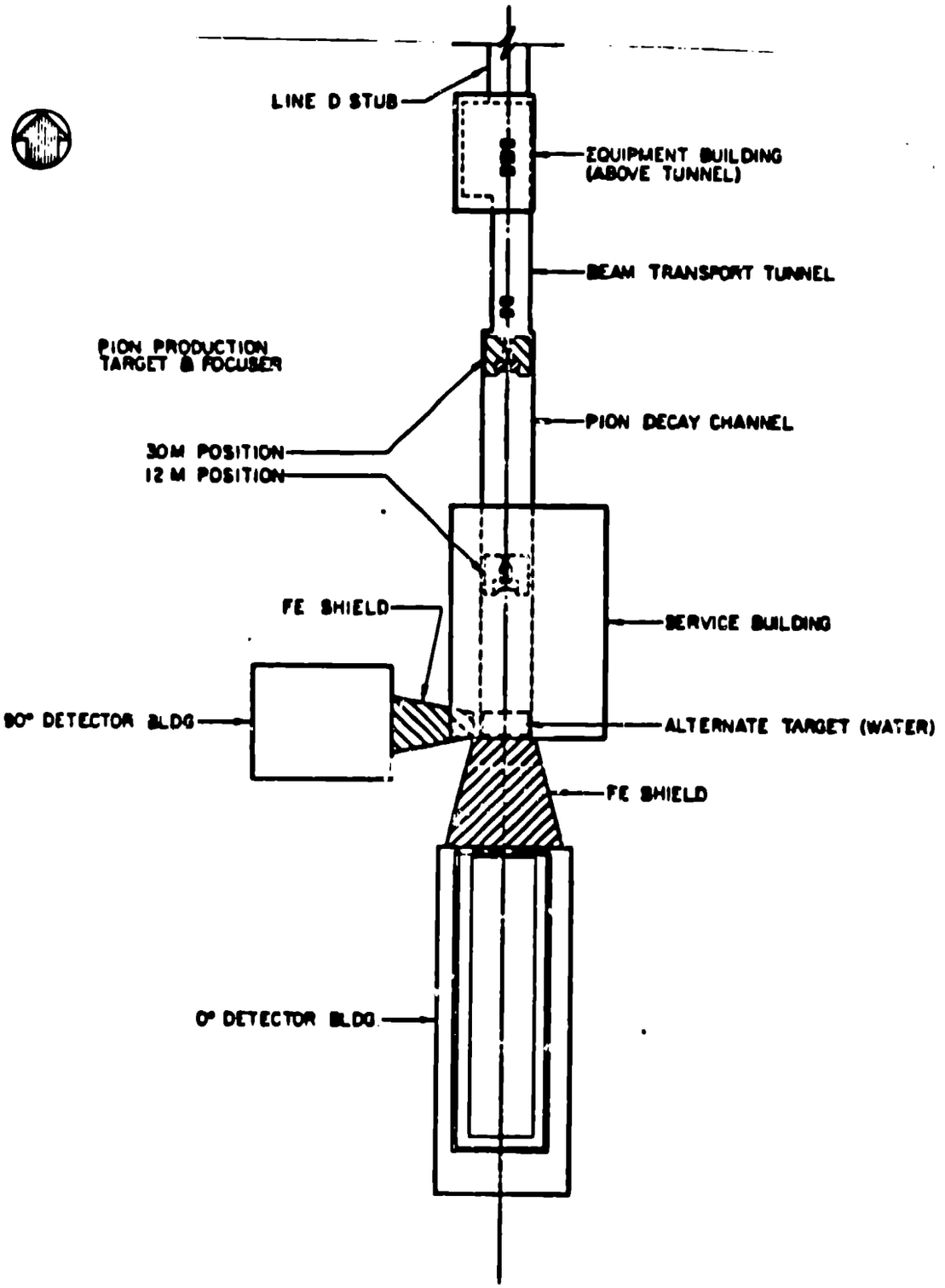

0 10 20 METERS
0 20 40 60 FEET

PROPOSED
NEUTRINO RESEARCH FACILITY

JANUARY 1982

Fig. 3

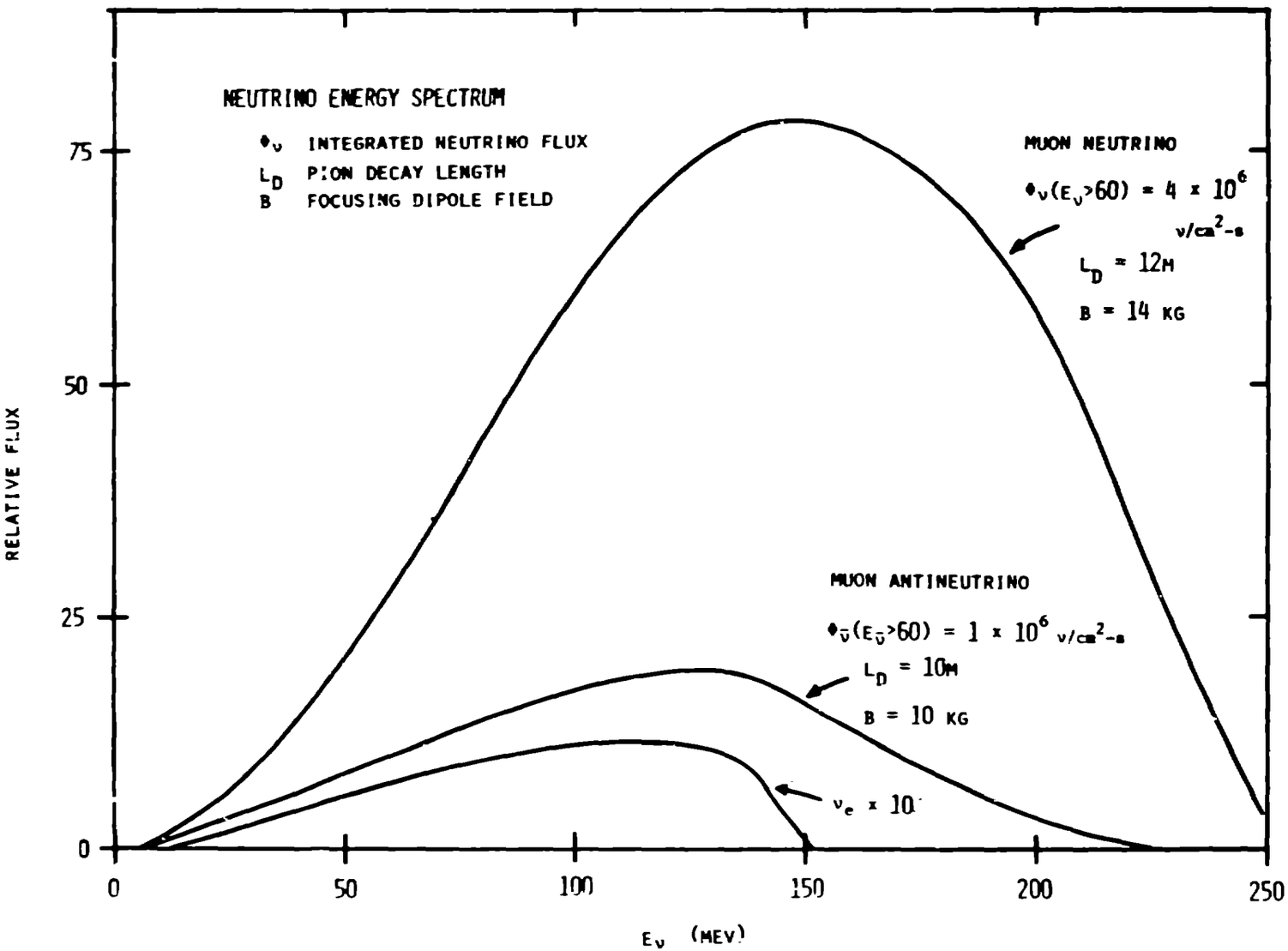
NEUTRINO ENERGY SPECTRUM
Φ_ν INTEGRATED NEUTRINO FLUX
L_D PION DECAY LENGTH
B FOCUSING DIPOLE FIELD
MUON NEUTRINO
$\Phi_\nu(E_\nu>60) = 4 \times 10^6$ ν/cm^2-s
L_D = 12M
B = 14 KG
MUON ANTINEUTRINO
$\Phi_{\bar{\nu}}(E_{\bar{\nu}}>60) = 1 \times 10^6$ ν/cm^2-s
L_D = 10M
B = 10 KG
$\nu_e \times 10$
RELATIVE FLUX
75
50
25
0
0
50
100
150
200
250
E_ν (MEV)

FIG. 4

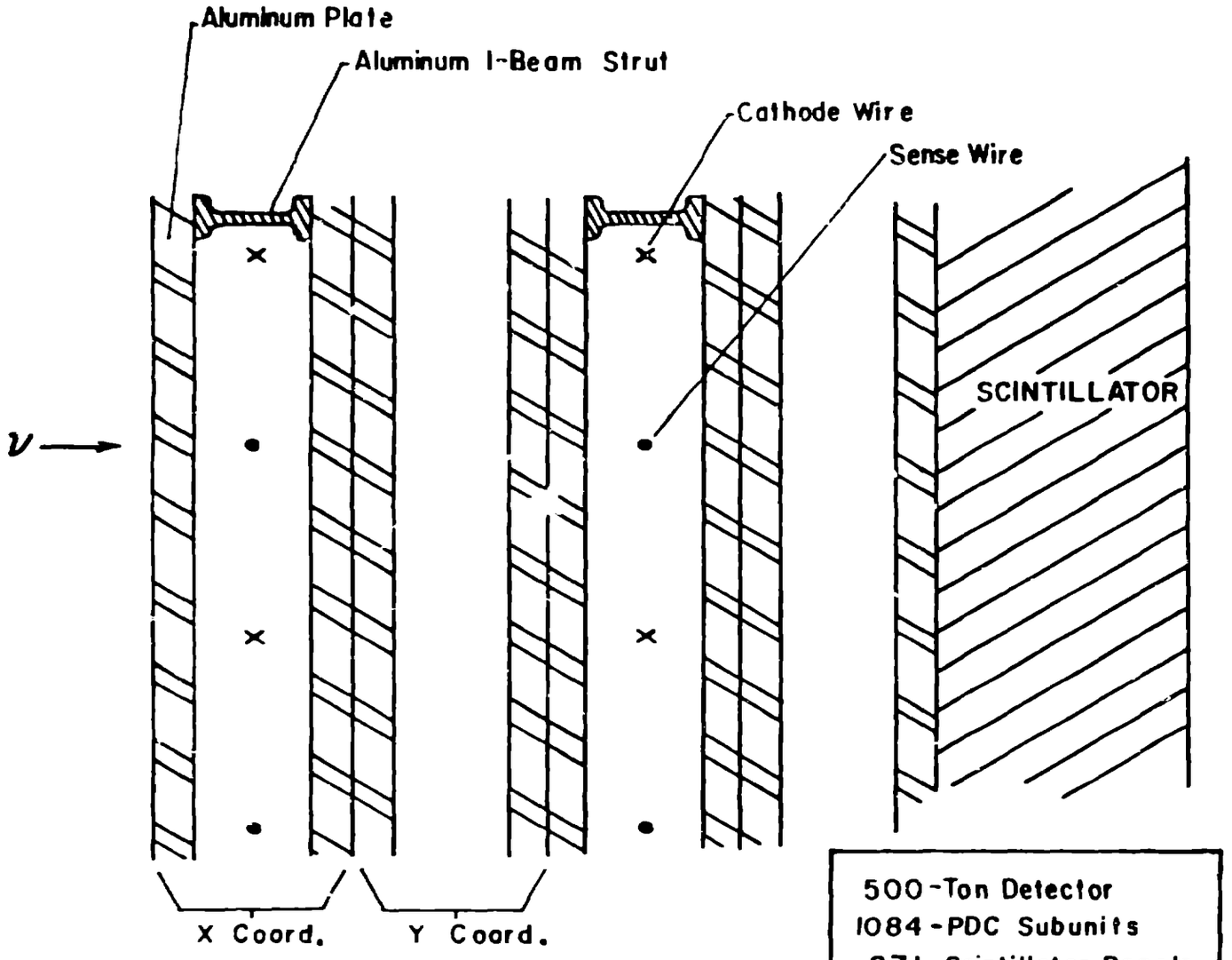
Aluminum Plate
Aluminum I-Beam Strut
Cathode Wire
Sense Wire
SCINTILLATOR
ν
X Coord.
Y Coord.
500-Ton Detector
1084-PDC Subunits
271-Scintillator Panels
PROPORTIONAL DRIFT CHAMBER (PDC)
SUBUNITS
Scale 1cm

FIG. 5

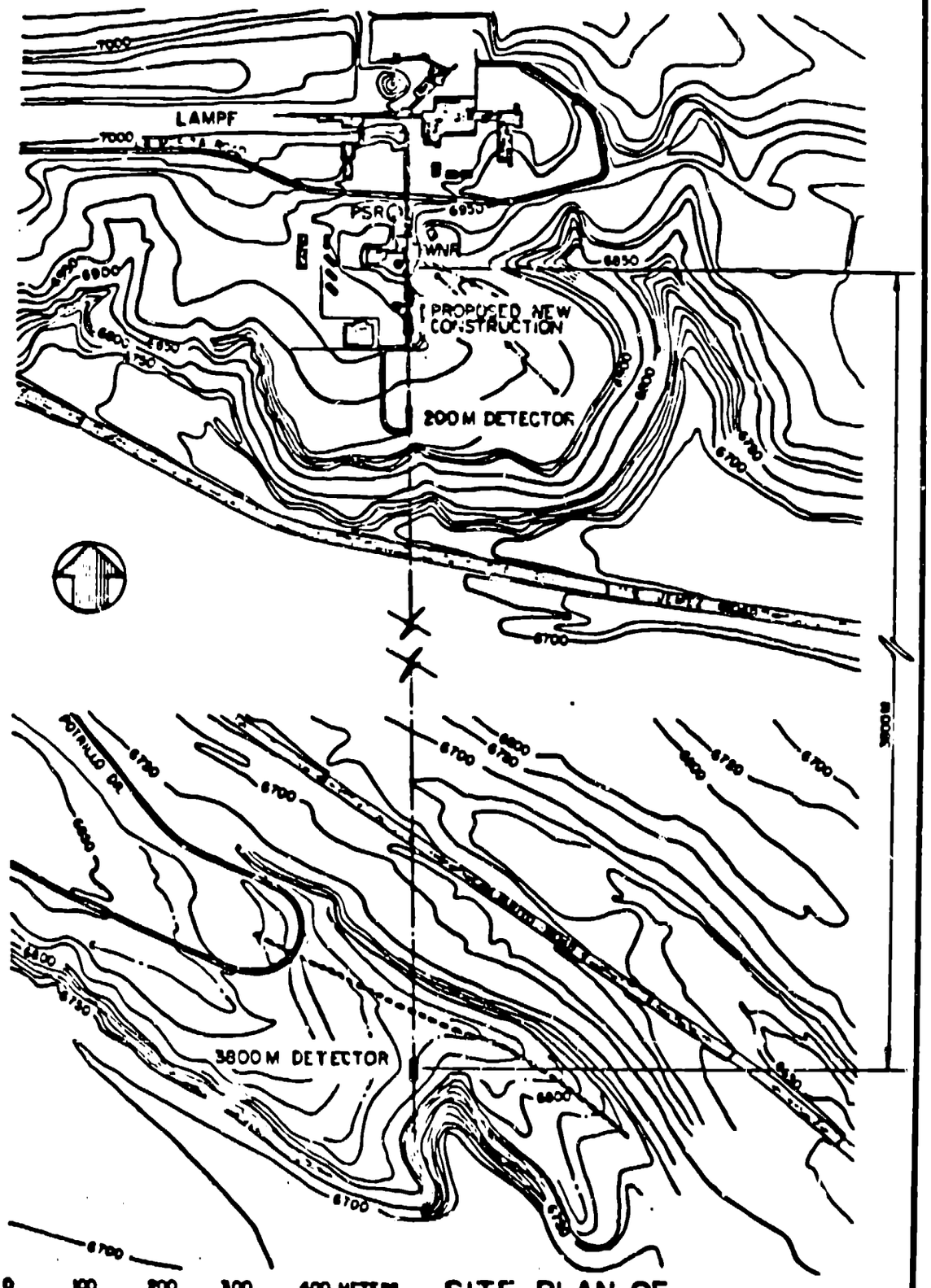
LAMPF
PSRC
WNR
PROPOSED NEW CONSTRUCTION
200 M DETECTOR
3800 M DETECTOR
POTRERO DR.
6700
6750
6800
6850
6900
7000
100 200 300 400 METERS
400 800 1200 FEET
SITE PLAN OF PROPOSED NEUTRINO RESEARCH FACILITY
JANUARY 1982

Fig. 6

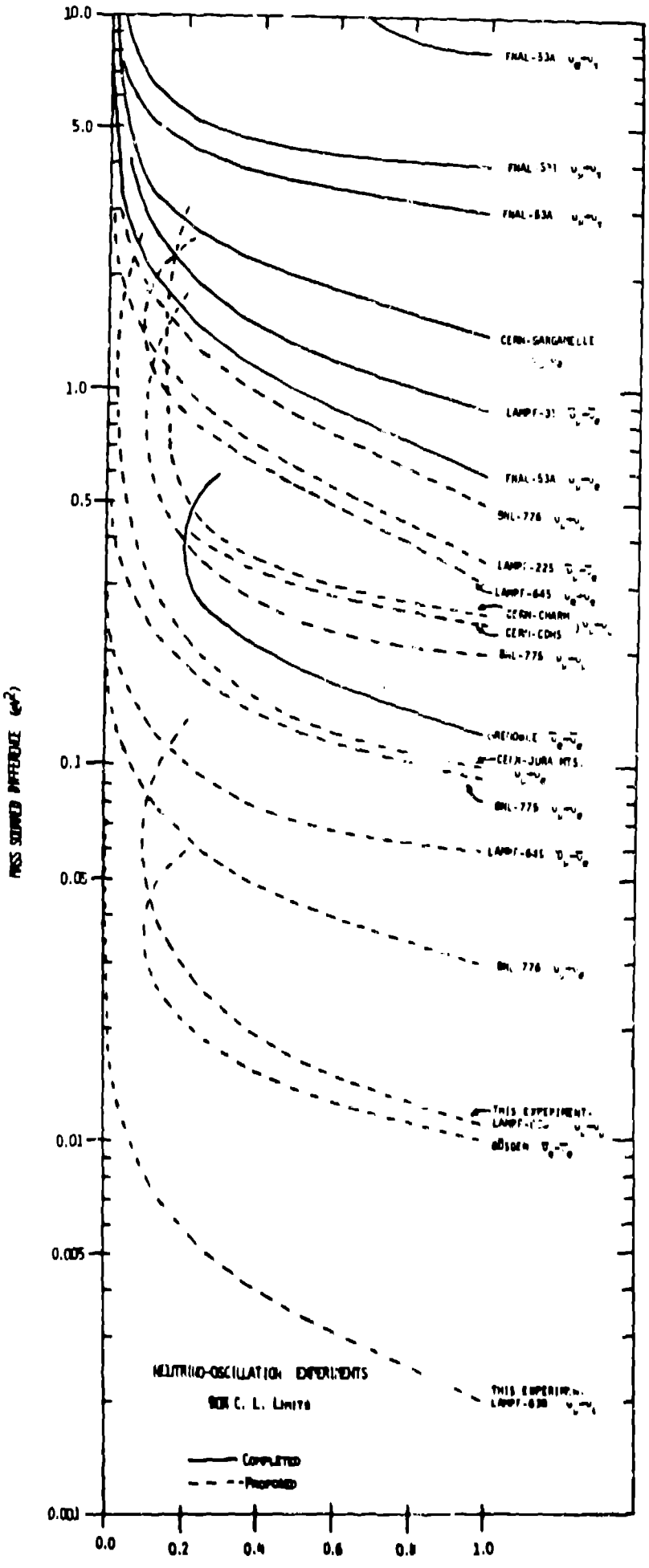
10.0
5.0
1.0
0.5
0.1
0.05
0.01
0.005
0.001
0.0
0.2
0.4
0.6
0.8
1.0
MASS SQUARED DIFFERENCE (eV²)
FNAL-53A
FNAL 531
FNAL-83A
CERN-GARGAMELLE
LAMPF-31
FNAL-53A
SNL-776
LAMPF-225
LAMPF-645
CERN-CHARM
CERN-CDHS
BNL-775
CHOOZ
CERN-JURA MTS.
BNL-775
LAMPF-645
BNL 776
THIS EXPERIMENT
LAMPF
BUGEY
THIS EXPERIMENT
LAMPF-030
NEUTRINO-OSCILLATION EXPERIMENTS
90% C. L. LIMITS
COMPLETED
PROPOSED